CNRS
Centre National de la Recherche Scientifique

INFN
Istituto Nazionale di Fisica Nucleare

Rough evaluation for the Automatic Alignment control noise in the SVC configuration

VIR-0285A-11

M. Mantovani

Issue: 1

Date: May 9, 2011

VIRGO * A joint CNRS-INFN Project
Via E. Amaldi, I-56021 S. Stefano a Macerata - Cascina (Pisa)
Secretariat: Telephone (39) 050 752 521 * FAX (39) 050 752 550 * Email W3@virgo.infn.it

Contents

1 Introduction **2**

2 Requirements **3**

3 Radiation pressure effect on the Mechanical TF **4**
3.1 Automatic Alignment control scheme 5
3.1.1 Sensing and Control 5
3.1.2 Control Noise 7

4 Conclusions **10**

5 Acknowledgements **10**

A Angular DOF reconstruction quality **11**

1 Introduction

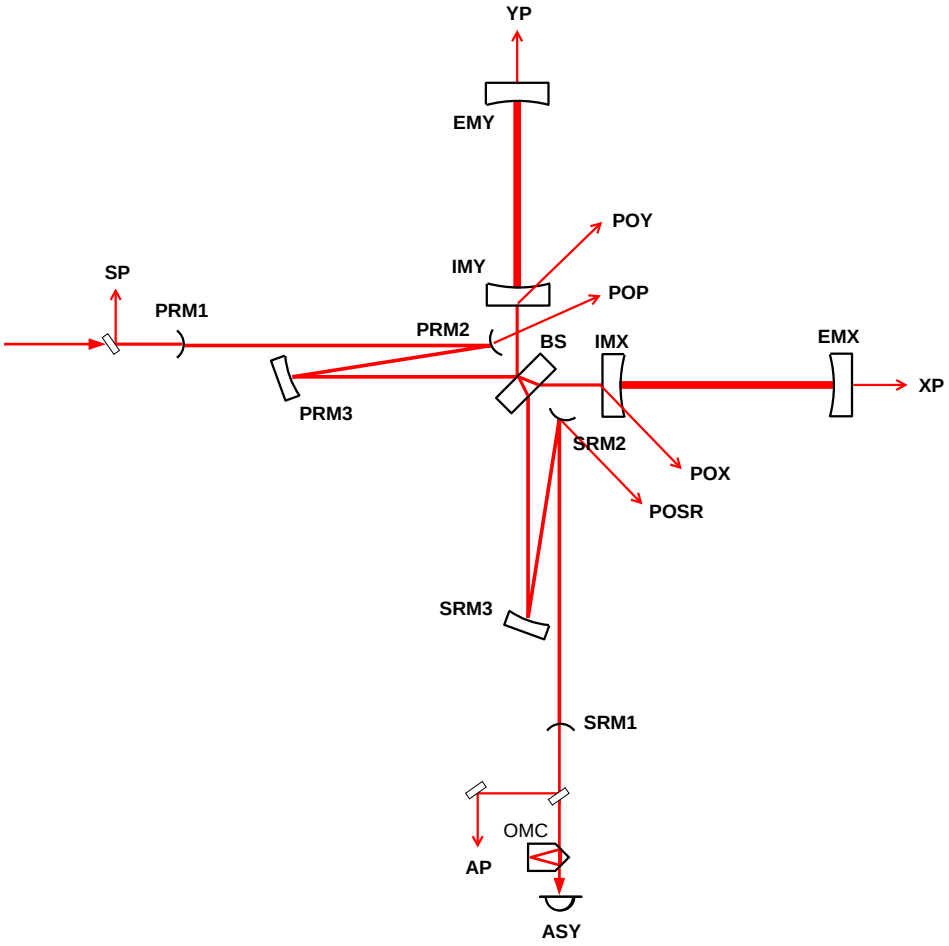

Figure 1: Optical layout for the Advanced Virgo interferometer in the Non Degenerate Recycling Cavities configuration. The detection ports are pointed by the red arrows.

PRM1 ROC	1.8175 m	PRM2 ROC	1.8175 m	PRM3 ROC	15.081 m
SRM1 ROC	1.8118 m	SRM2 ROC	1.8118 m	SRM3 ROC	14.314 m
PRCL1	6.780 m	PRCL2	6.780 m	PRCL3	10.703 m
SRCL1	6.473 m	SRCL2	6.395 m	SRCL3	10.686 m

Table 1: Optical parameter for the Signal Recycling Cavity and the Power Recycling cavity.

For the Advanced Virgo optical design two main configurations are proposed: the **MSRC** [1], Marginally Stable Recycling Cavities design, and the **SVC** [2], Short Vertical Cavities, design which is the last design for Non-Degenerate Recycling Cavities where thee three mirrors for the PRC and SRC are displaced in the Z configuration with double vertical payload suspensions [3].
The Automatic Alignment control scheme and noise performance have been evaluated for the MSRC case [4] while it can not be simulated for the SVC case since the Mechanical TF for the RM1/3 mirror suspension is not available yet. In this note the control noise for the SVC design has been extrapolated starting from the assumption, which it is very optimistic, that the suspension performance for the double-payload is the same of the present Super-Attenuator.

2 Requirements

The requirements for the angular and transversal mirror displacement have been evaluated as [5]:

mirror (tilt)	RMS [μrad]	mirror	RMS [μrad]	mirror	RMS [μrad]
PRM1	5	PRM2	0.5	PRM3	0.05
SRM1	2	SRM2	0.25	SRM3	0.03
mirror (shift)	RMS [μm]	mirror	RMS [μm]	mirror	RMS [μm]
PRM1	9	PRM2	0.9	PRM3	0.75
SRM1	3.6	SRM2	0.45	SRM3	0.43

Table 2: Requirements for the Recycling cavity mirrors for the NDRC SVC design.

It is important to notice that the requirements on the transversal directions, vertical and horizontal, are very stringent and they imply the development of a transversal direction control for the mirrors which has never been studied and implemented in the present first generation of gravitational wave interferometer.

3 Radiation pressure effect on the Mechanical TF

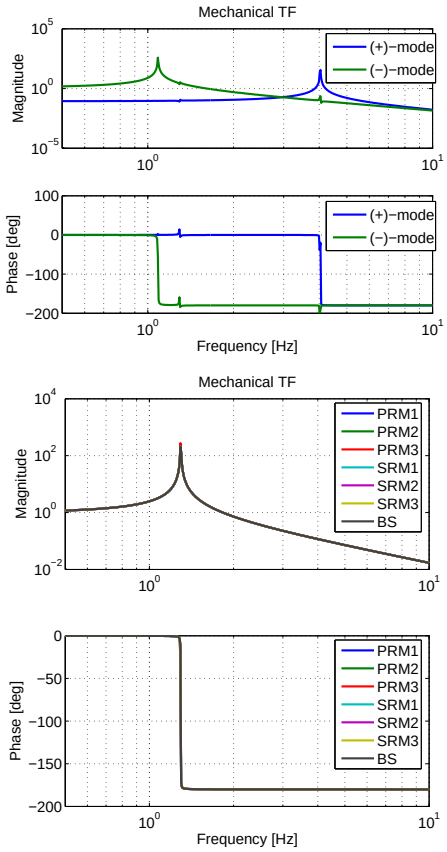

Figure 2: Mechanical Transfer functions for the interferometer angular degrees of freedom. In the top plot the Transfer functions for the arm cavity modes, (+) and (-) modes, for 125 W of input power, are shown. The (+)-mode raises strongly the resonance frequency due to the radiation pressure effect while the (-)-mode slightly decreases. The bottom plot shows the mechanical transfer functions for the central cavity mirrors (the power recycling mirrors PRM1/2/3; the signal recycling mirrors SRM1/2/3; and the Beam Splitter mirror BS). Since the power stored in the central area is low the mechanical TF are not modified by the radiation pressure optical spring.

The mechanical transfer function of the angular degrees of freedom can be simulated by *Optickle*[6] as it is shown in Figure 2.
As expected the arm cavity TF are completely changed: the (+)-modes transfer function has a resonant frequency of 4.035 Hz starting from 1.239 Hz; the (-)-mode eigen-frequency is reduced to 1.085 Hz, remaining stable. Instead the central cavity mirrors are not affected by the radiation pressure due to the low power impinging on the mirrors.
The change of the Mechanical Transfer Functions has to be taken into account in the control filter design, where the whole suspension TF has been taken into account.

3.1 Automatic Alignment control scheme

In order to design the Automatic Alignment control scheme the alignment error signals have been simulated at each detection port shown in Figure 1.
For the Automatic Alignment three phase modulation frequencies have been used:

- **SB1** which is resonating in the PR and SR cavities
- **SB2** which is resonating only in the SR cavity
- **SB3** which does not enter in the ITF

Which allows to have the demodulation frequencies as: DC, f1, f2, f3, plus the beat between them (as the f2-f1. f3-f2 and f3+f1). Plus the 2×f2 for the AP quadrants beam centering.
In order to design a working control scheme the amplitude of the TF between the angular degree of freedom and the quadrant diodes has been simulated.
At each detection port two quadrant diodes, one in near field (XX_A) and one in far field (XX_B), are placed. The quadrants have to be suspended in vacuum to reduce the spoiling of the signals, both RF and DC. For more details see the Virgo note [4].
The sensing has been constructed by tuning the demodulation and the Gouy phases.
The power impinging on each quadrant diode is 25 mW, considering to have a maximum acceptable impinging power of 50 mW [1] except for the AP quadrant diodes which are set to 2.5 mW of impinging power [2].
In the following the absolute amplitude of the error signal, in W/mrad, is shown for each detection port maximizing the amplitude tuning the Gouy phase and the demodulation phase, which are expressed in degrees. The largest amplitudes are marked in bold.
Moreover in the following, for lay out reasons, D+, D-, C+ and C- will be Differential(+), Differential(-), Common(+) and Common(-).

3.1.1 Sensing and Control

In this section the sensing, thus the control, scheme for the Automatic Alignment will be detailed.
In the Advanced Virgo SVC configuration not all the angular degrees of freedom can be globally controlled. The Power recycling cavity, for instance, is a folded cavity and the folding mirror can not be globally controlled since the d.o.f. can not be independently sensed. The PRM2 can not be decoupled from the PRM3 since the error signal has the same behavior of the PRM3 signal as a function of the demodulation and Gouy phases, but with lower signal amplitude. The same for the signal recycling mirrors. Moreover since the accuracy requirements for the RM1 mirrors are quite relaxed these d.o.f. will be controlled in Drift control mode and they can be ignored in the control noise analysis since they will not contribute strongly to the control noise.
The angular modes which will controlled with the Fast Control mode (∼1 Hz of bandwidth) are:

- the arm cavity d.o.f.: Differential(+), Differential(-), Common(+) and Common(-)
- the power recycling mirror PRM3
- the Beam Splitter mirror BS
- the signal recycling mirror SRM3

[1] This value is not finalized yet, but since for V+ the high power quadrant diodes can accept 30 mW of impinging power, a maximum tolerance of 50 mW could be feasible.
[2] The maximum allowed beam power for the AP quadrants is 2.5 mW to be more conservative and pessimistic since it is not clear up to now which is the amount of power at the dark port which will be used for angular control. Of course if the amount of power will be higher the sensing noise will decrease as the square root of the impinging power.

	D+	D-	C+	C-	PRM3	SRM3	BS
AP_B fm2 ϕ_G= 44 ϕ_{dem}=79	**-5.9693**	**3.1392**	0.0180	0.0162	-0.8205	0.8049	-0.6942
$TRA_{(-)}$ DC ϕ_G= 81 for YP and XP	0.1518	**-3.9907**	0	-0.0290	0.0001	-0.0005	0.0081
SP_B fm3 ϕ_G= 155 ϕ_{dem}=139	-0.0034	-0.2324	**-5.8001**	**3.1789**	-0.2024	0	-0.3682
$TRA_{(+)}$ DC ϕ_G= 78 for YP and XP	0	-0.0291	0.1470	**-3.9888**	-0.0197	0	-0.0070
SP_A fm3 ϕ_G= 65 ϕ_{dem}=135	0.0029	0.00248	0.09175	0.18577	**-0.85734**	0	**-0.29625**
SP_B fm2 ϕ_G= 134 ϕ_{dem}=9	**1.6000**	**1.4813**	0.0061	-0.0184	**-1.1294**	**1.2106**	-0.0367
POP_B fm2 ϕ_G= 113 ϕ_{dem}=0	0.01575	**0.25403**	-0.06738	-0.07356	**0.26553**	**0.13677**	**0.38013**

Table 3: Sensing scheme for the high power, i.e. 125 W, ITF with SR cavity. The strongest elements are highlighted in bold.

Where in the first column the diodes used for the sensing and the demodulation frequencies are shown. The diode names follow the nomenclature shown in Figure 1 and the $TRA_{(+)}$ DC and $TRA_{(-)}$ DC are the sum of the DC signals of the diodes placed in transmission to the cavities (XP ad YP). In the first row the angular d.o.f. sensed are labeled, they are Differential plus, Differential minus, Common plus, Common minus, PRM3, SRM3 and BS respectively.
The sensing scheme has been built choosing the signals which allows the best decoupling of the angular d.o.f. taking into account not to spoil the signal to noise ratio, in other words that the stronger signals have been chosen.
As it is shown in Table 3 the sensing is not well decoupled and due to the fact that the angular requirement for these mirrors are stringent a hierarchical control can not be applied even if it would help in decoupling the sensing.
The control scheme is then:

- **Differential(+)** controlled by using the dark port quadrant demodulated at fm2.
- **Differential(-)** controlled by using the difference of the DC signals of the arm cavity transmitted signals.
- **Common(+)** controlled by using the symmetric port quadrant demodulated at fm3.
- **Common(-)** controlled by using the sum of the DC signals of the arm cavity transmitted signals.
- **PRM** controlled by using the symmetric port quadrant demodulated at fm3.
- **BS** controlled by using the pick-off beam POP demodulated at fm2.

The control matrix is then computed by inverting the sensing.

	AP_B fm2	$TRA_{(-)}$ DC	SP_B fm3	$TRA_{(+)}$ DC	SP_A fm3	AP_B fm2	POP_A fm2
D+	**1.0000**	**0.5994**	0	0	**1.1766**	**-0.9747**	**2.7431**
D-	0	**1.0000**	0	0	0	0	0
C+	0	0	**1.0000**	**0.7970**	0	0	0
C-	0	0	0	**1.0000**	0	0	0
PRM3	0	0	0	0	**1.0000**	-0.1148	**0.8355**
SRM3	**-0.2680**	0	0	0	**-1.5981**	**1.0000**	**-1.7350**
BS	0	0	0	0	**0.4555**	-0.1374	**1.0000**

Table 4: Control matrix. The strongest elements are highlighted in bold. The control matrix has been normalized on the diagonal elements to enhance the visibility of the off diagonal coupling.

The designed control scheme is not diagonal. It has to be noticed that in the control matrix the small elements in each row (at least 10 times lower than the stronger element in the row) are nulled.

3.1.2 Control Noise

In order to evaluate the control noise the *Pickle* tool of *Optickle* [7] has been used considering as input noise only the shot noise of the quadrant diodes and the seismic noise at the optics level. It allows to evaluate the residual angular motion of the mirrors and the control noise contribution in the sensitivity.

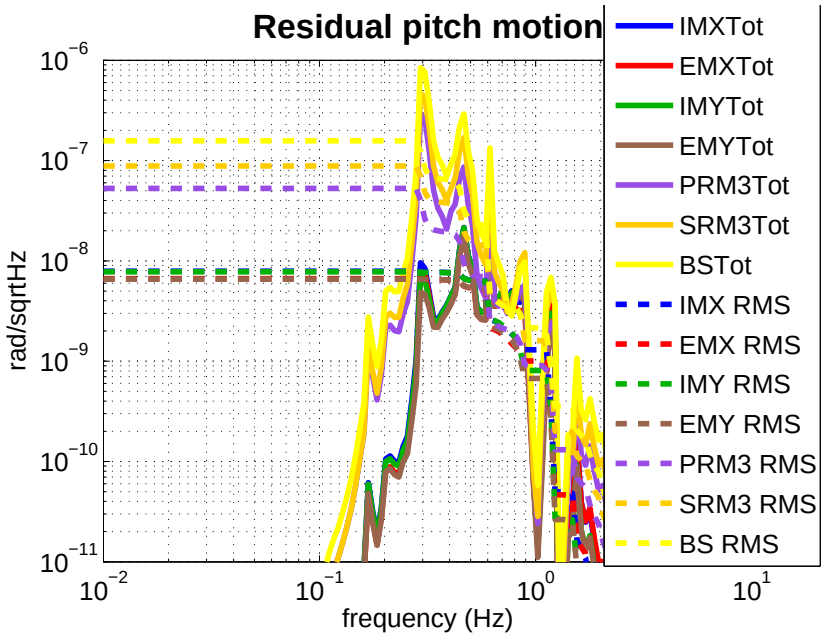

Figure 3: Residual motion. The RMS of the arm cavity mirrors is not compliant with the requirements but it should be achievable by tuning the filtering.

The low frequency part of the filtering has not been optimized to match perfectly the requirements, to do not spend to much time in curing resonances etc.., but only to be at a factor ∼2 from the requirements, as it was done for the MSRC case.

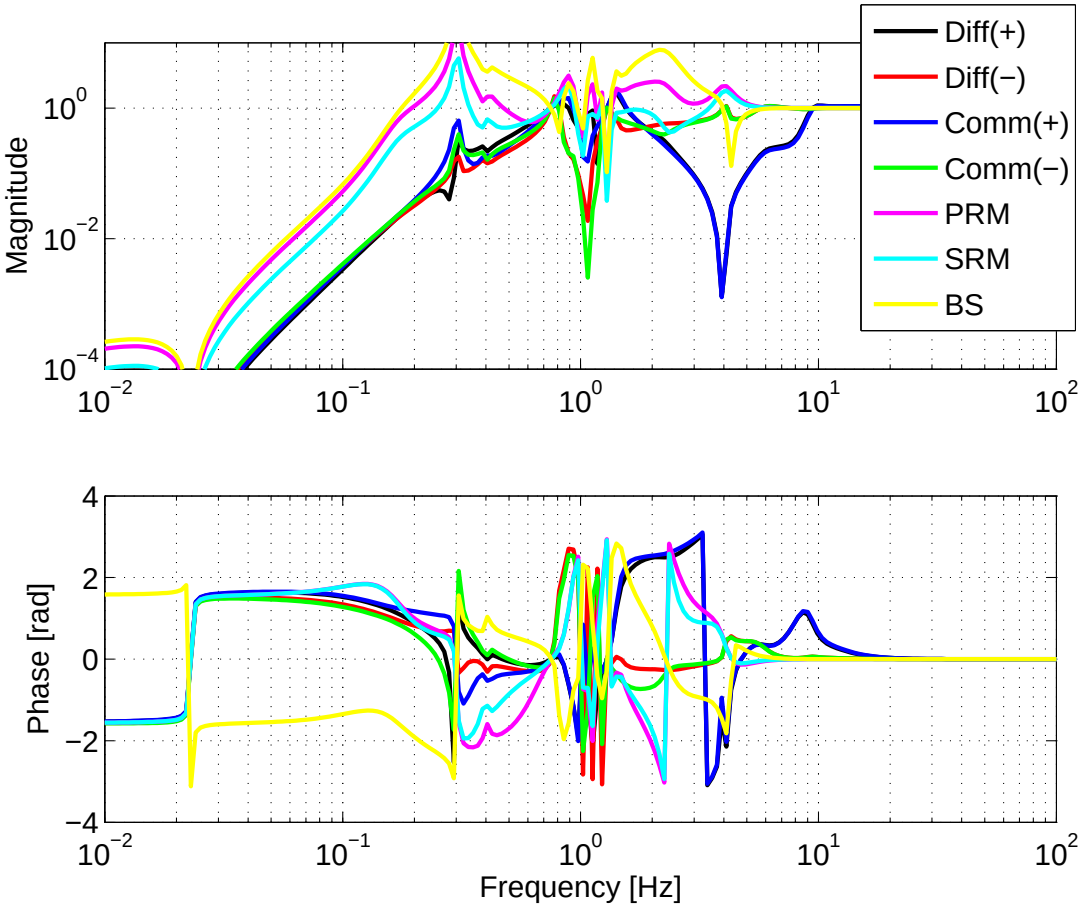

Figure 4: Control filtering closed loop TF.

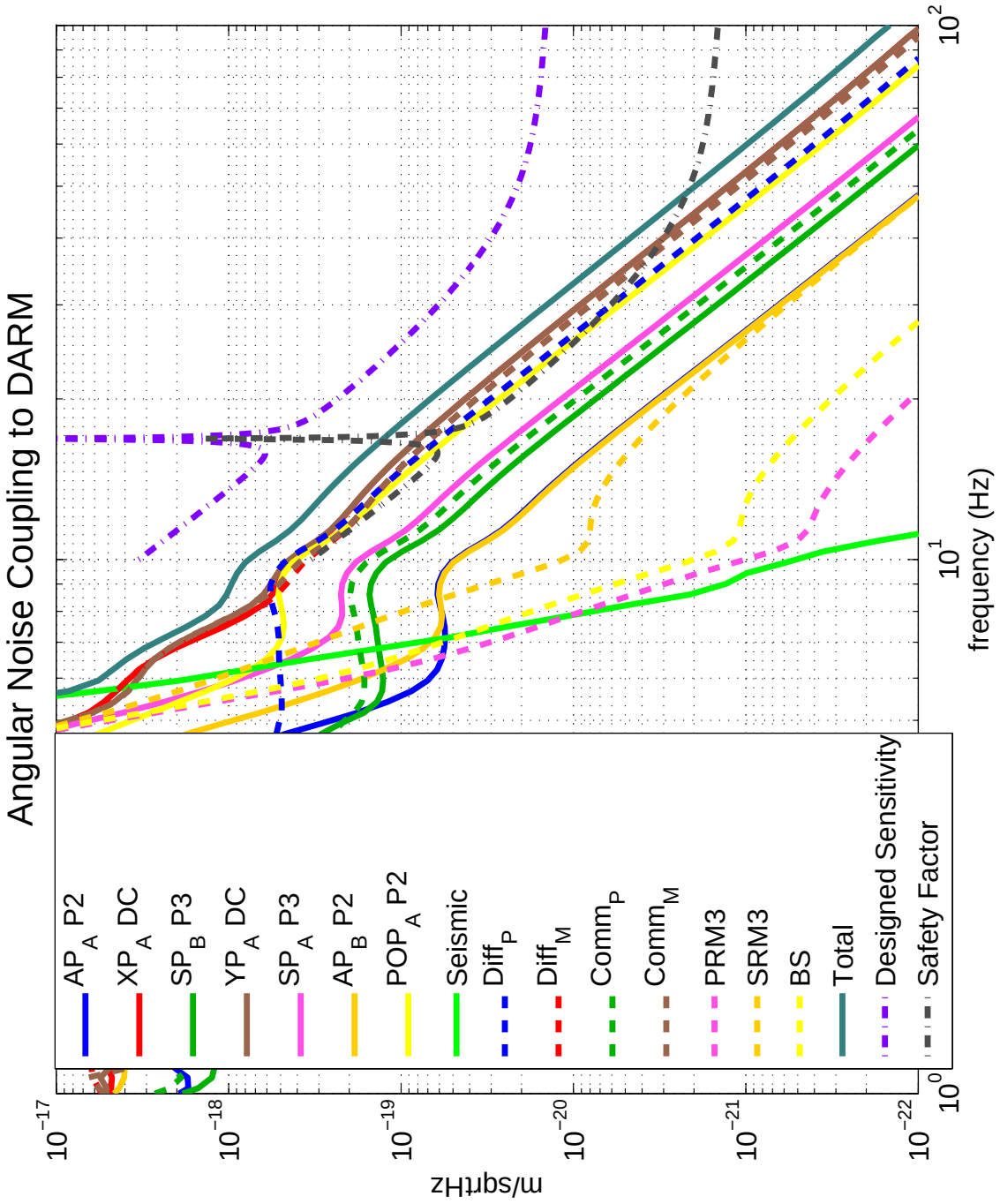

Figure 5: Angular control noise contribute in the sensitivity. It results to be compliant with the safety factor (10 times below the design sensitivity).

As it is shown in Figure 5 the control noise is not fulfilling the safety factor requirements, 10 times below the design sensitivity, mostly because the control is strongly coupled and the sensing is weaker due to the stability of the recycling cavities.
The strong coupling spoils the control of important d.o.f. as the Differential(+) mode, as it is shown in Table 4, increasing the control noise. This fact is well visible looking at the angular noise budget in which the noise given by each diode does not coincide with the control noise of each angular mode.
Moreover in this analysis the coupling with the mirror transversal displacement, vertical and horizontal, have been neglected even if it is fundamental.

4 Conclusions

A speculation on the angular control noise in case of Short-Vertical recycling cavities has been done in this note. It is only a rough evaluation since the mechanical TF for the double vertical payload, which suspends the RM1/3 mirrors, is not available yet and it has been assumed that it will have the same performances of the present Super-Attenuator.
As it is shown in the Section 3.1.1, the sensing is weaker and more coupled with respect to the MSRC case due to the stability of the recycling cavities and it will cause excess of noise in the most critical d.o.f. as the Differential Plus mode.
The decoupling of the system would be obtained by engaging the SRM3 with lower control bandwidth, a hierarchical control as it is planned for the MSRC case, but it is not possible since the accuracy requirement for the SRM3 is stringent and not achievable with the Drift control.
An other important aspect, that it has not been taken into account in this note, is the strong coupling between the angular and the transversal directions, due to short radii of curvature chosen for the recycling mirrors, which will disturb the control, see the Virgo note [8].

5 Acknowledgements

This research activity has been partially supported by Regione Toscana (Italy) through the program POR CreO FSE 2007-2013 of the European Community, within the project n. 18113 (ISAV).

A Angular DOF reconstruction quality

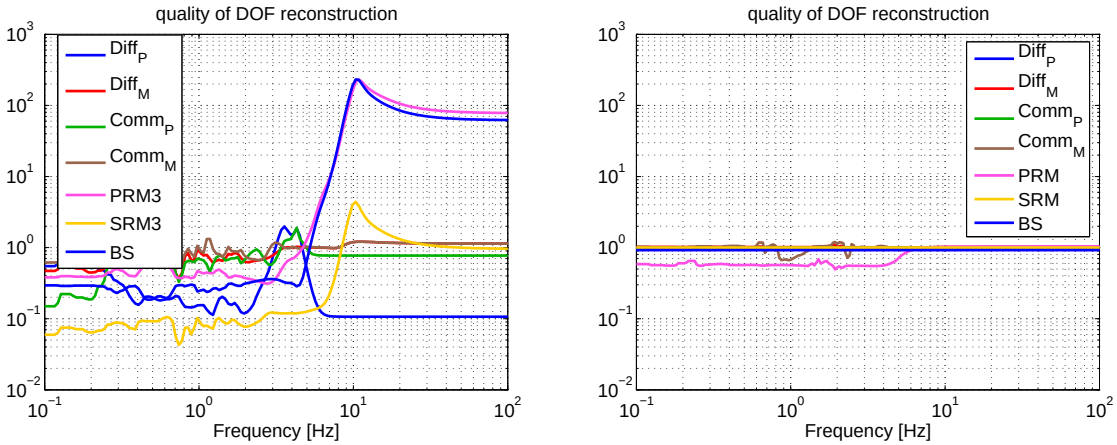

Figure 6: Angular d.o.f. reconstruction quality for the SVC configuration on the left and for the MSRC configuration on the right. The value 1 means angular perfectly reconstructed. From the plot it is clear that the MSRC configuration has a much better reconstruction quality.

As it has been pointed out in the note, one side effect of the weakness and of the strong coupling of the signal is the fact that the angular d.o.f. are not well reconstructed. The quality of the reconstruction of the signals can be evaluated thanks to the ratio between the diode noise and the angular mode noise. From Figure 6 it is clear that in the MSRC configuration the angular d.o.f. reconstruction is much better with respect to the SVC configuration.

References

[1] J. Marque et al., "AdV design: MSRC case", VIR-0128A-11 2

[2] M. Barsuglia, R. Flaminio, M. Granata, B. Mours, R. Ward, "New optical layout for stable recycling cavities", VIR-0452A-10 2

[3] J. Van den Brand et al., "DOUBLE VERTICAL PAYLOADS On-axis suspension of power and signal recycling mirrors", VIR-0145A-11 2

[4] M. Mantovani, "Automatic Alignment Sensing and Control scheme for Advanced Virgo MSRC configuration", VIR-0201A-11 2, 5

[5] M. Mantovani, "Stable Recycling Cavities : L.R.C. vs S.R.C. angular requirements ", VIR-0029B-11 3

[6] Optickle home-page *http : //ilog.ligo − wa.caltech.edu : 7285/advligo/ISC_Modeling_Software* 4

[7] L. Barsotti, M. Evans, "Modeling of Alignment Sensing and Control for Advanced LIGO", LIGO-T0900511-v4 7

[8] M. Mantovani, "Draft Automatic Alignment Sensing and Control scheme for Advanced Virgo", VIR-0323A-10 10